Electronic Supplementary Material (ESI) for New Journal of Chemistry.

Facile preparation of $V_2C@VO_x$ nanosheets with excellent multi-enzyme activity and their colorimetric sensing application

Haiyan Wang[a,b,c]*, Cheng Liu[b], Yue Zhao[b], Xinyu Luo[b], Pengjie Yin[b], Fuyou Du[b]* and Guangsheng Zeng[a,b,c]*

[a] *Hunan Engineering Research Center of Research and Development of Degradable Materials and Molding Technology, Changsha University, 410022, China*

[b] *College of Biological and Chemical Engineering, Changsha University, Changsha 410022, China*

[c] *Hunan Provincial engineering research center for modification and processing of low-carbon degradable materials, Changsha University, 410022, China*

* Corresponding author: Tel: +86-84261506; Fax: +86-731-84261382;

E-mail address: wanghaiyan@ccsu.edu.cn (Haiyan Wang), dufu2005@126.com (Fuyou Du), guangsheng_zeng@126.com (Guangsheng Zeng)

Tab. S1. Comparison of synthesized methods of nanoenzymes.

Nanoenzymes	synthesized method	synthesized condition	Ref.
$CoPW_{11}O_{39}$	immersion method	refluxed at 80 ºC for 2 h	[1]
poly(ethylene glycol) diacrylate	photolithography	enzyme, redox mediator and photoinitiator	[2]
$SnFe_2O_4$ nanoparticles	hydrothermal method	heated to 200 °C for 15 h	[3]
Co–Fe nanoparticles	hydrothermal method	heated at 200 °C for 12-14 h	[4]
MOF@COF hybrid nanozymes	solvothermal method	sequential growth	[5]
Co-Fc@GOx	hydrothermal reaction	sonicated for 30 min and heated at 120 °C for 3 h	[6]
$V_2C@VO_x$ nanosheets	hydrothermal method	heated at 140 °C for 2 h	This work

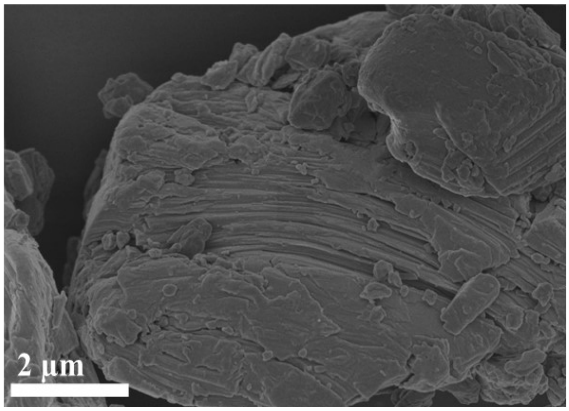

Fig. S1. The SEM image of V_2AlC.

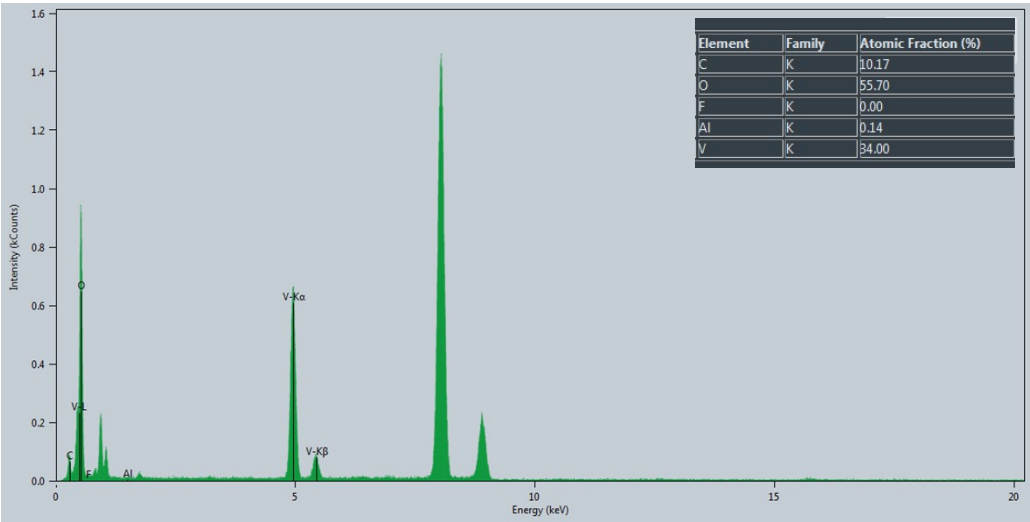

Fig. S2. The EDS analysis of $V_2C@VO_x$ nanosheets, inset is the atomic % of C, O, Al and V.

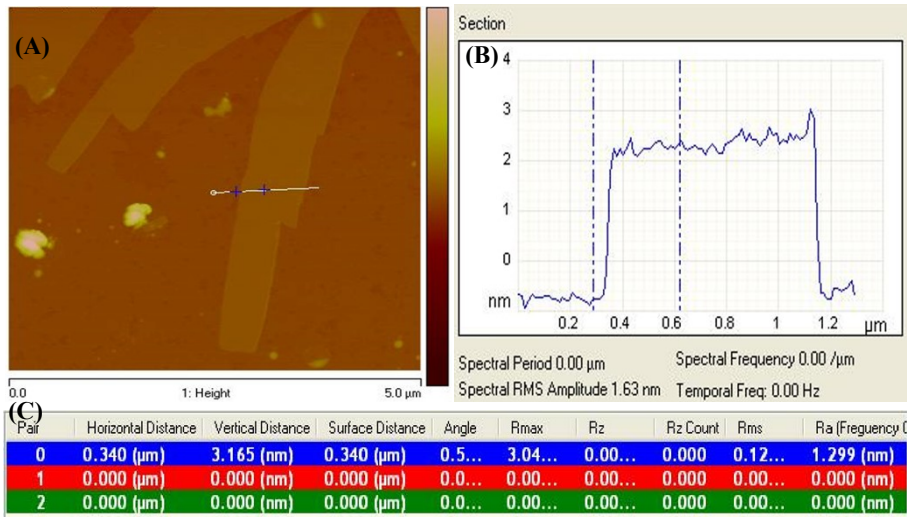

Fig. S3. (A) AFM image of as-synthesized $V_2C@VO_x$ nanosheets. (B) Their corresponding height image and (C) the data of vertical distance.

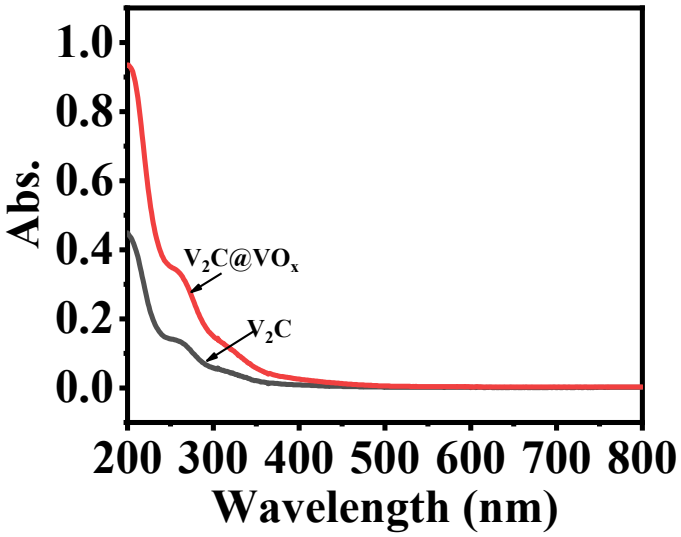

Fig. S4. UV-vis spectra of as-synthesized V_2C and $V_2C@VO_x$ nanosheets solution.

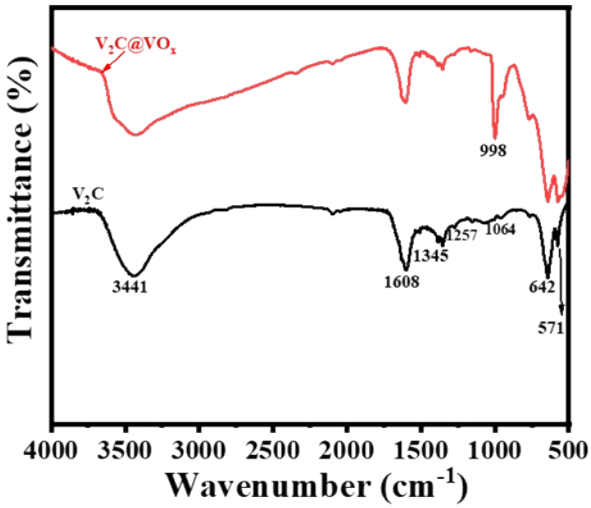

Fig. S5. FT-IR spectra of V_2C and $V_2C@VO_x$ nanosheets.

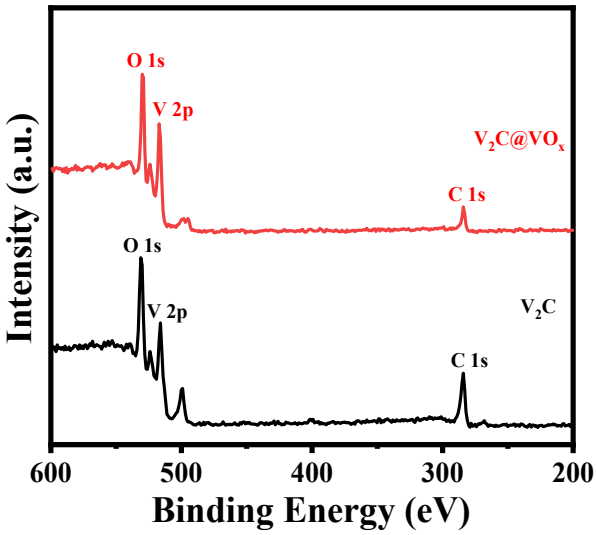

Fig. S6. XPS spectrum of V_2C and $V_2C@VO_x$ nanosheets.

Tab. S2. Content analysis of XPS fitted peaks for V_2C

	C1s	Atomic (%)	V2p	Atomic (%)	O1s	Atomic (%)
V_2C	O-C=O	11.28 %	V-C	13.96 %	V-C-O	98.6 %
	C-C	66.47 %	V^{4+} $p_{1/2}$	23.8 %	-OH	1.4 %
	C-O	16.6 %	V^{4+} $p_{3/2}$	62.24 %		
	C-V	5.65 %				

Tab. S3. Content analysis of XPS fitted peaks for $V_2C@VO_x$ nanosheets

	C1s	Atomic (%)	V2p	Atomic (%)	O1s	Atomic (%)
$V_2C@VO_x$ nanosheets	O-C=O	2.55 %	V-C	6.81 %	V-C-O	86.06 %
	C-C	72.5 %	V^{4+} $p_{1/2}$	25.97 %	-OH	13.94 %
	C-O	24.95 %	V^{4+} $p_{3/2}$	67.22 %		

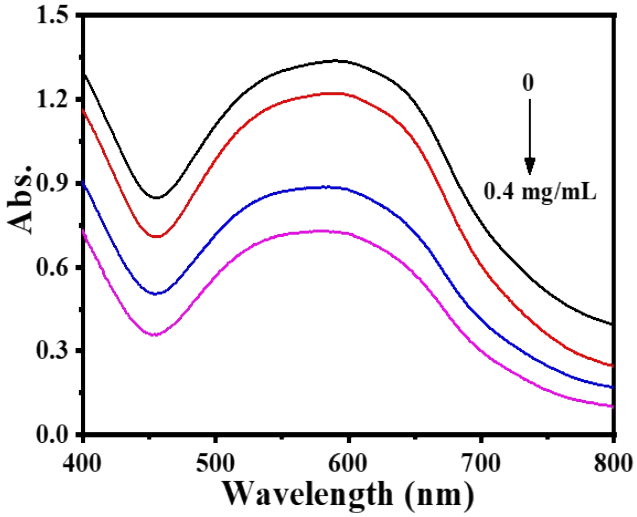

Fig. S7. The UV-vis spectra of NBT with different concentrations of $V_2C@VO_x$ nanosheets.

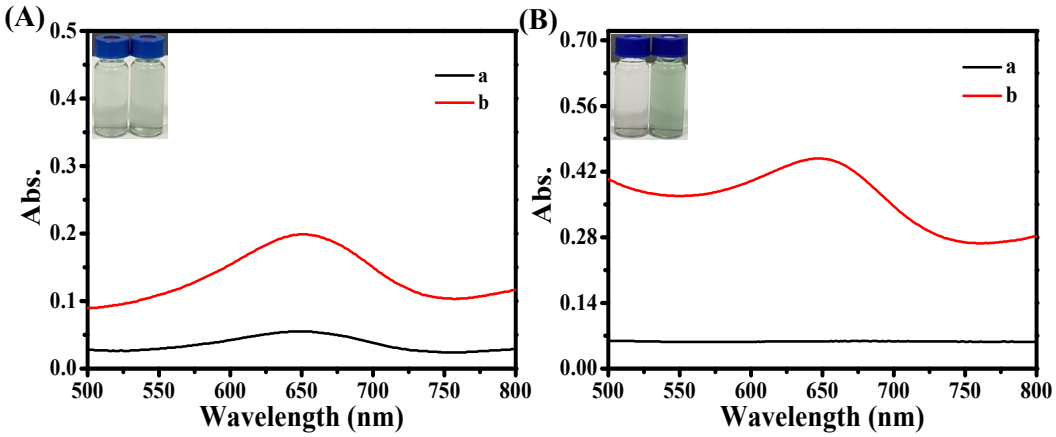

Fig. S8. (A) Absorption spectra of $V_2C@VO_x$ nanosheets (0.01 mg/mL)/TMB solution under air-saturated condition (a) and $V_2C@VO_x$ nanosheets (0.02 mg/mL)/TMB solution under air-saturated condition (b). (B) Absorption spectra of the solution containing TMB and $V_2C@VO_x$ nanosheets under N_2-saturated condition (a) and O_2-saturated condition (b).

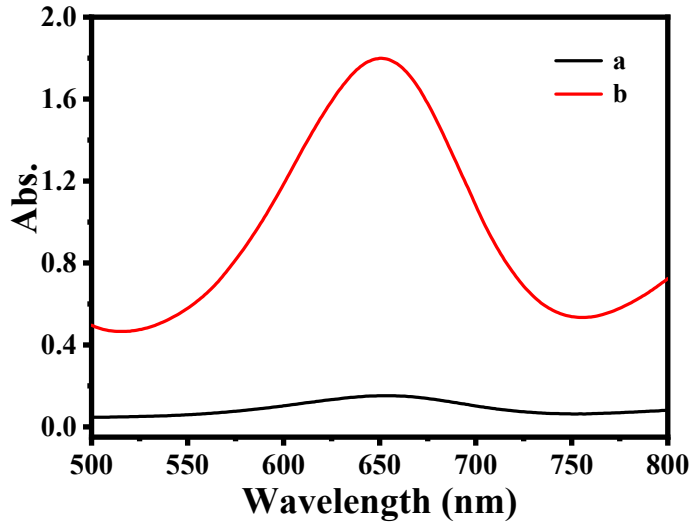

Fig. S9. The UV-vis spectra of (a) V_2C/TMB/H_2O_2 (1.5 mM) and (b) $V_2C@VO_x$/TMB/H_2O_2 (1.5 mM). [TMB]= 0.2 mM. [$V_2C@VO_x$]=0.02 mg/mL. [V_2C]=0.02 mg/mL. The above solutions were incubated in NaAc-HAc buffer (pH 4.0, 0.2 M) at 40 °C for 5 min.

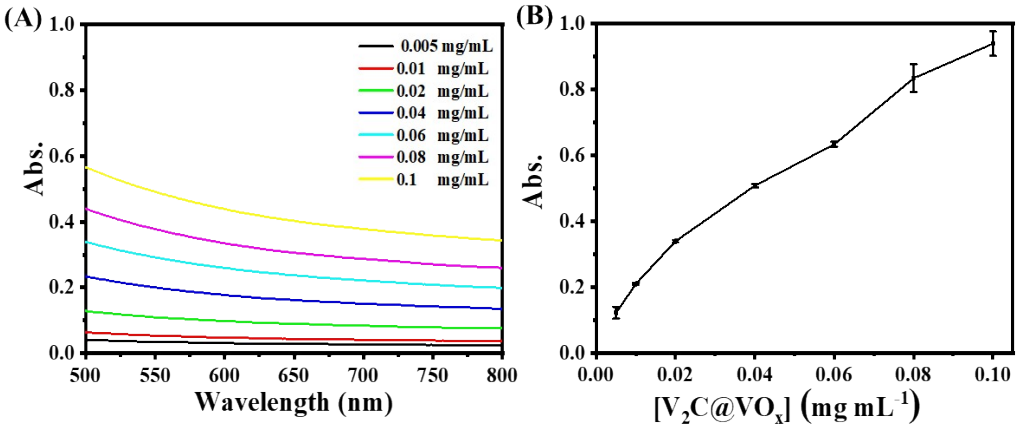

Fig. S10. UV-vis spectra for $V_2C@VO_x$ nanosheets of various concentrations. The optimum $V_2C@VO_x$ nanosheets concentration is 0.02 mg/mL for peroxidase-like activity.

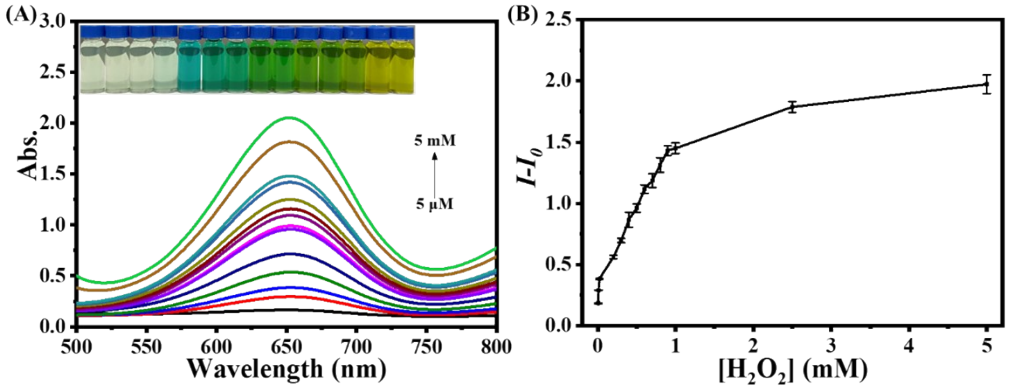

Fig. S11. (A) Under optimal conditions, UV-vis spectra of TMB interaction with different H_2O_2 concentrations. The inset image shows the corresponding photograph of the solutions containing different concentrations of H_2O_2. (B) The linear standard curve for H_2O_2 determination. Here, I_0 and I are defined as the maximum Abs. at 652 nm without or with H_2O_2, respectively.

Tab. S4. Comparison of the performances among various sensing materials for the glucose detection through a colorimetric approach.

Sensing materials	Linear range (μM)	LODs (μM)	Ref.
Microfluidic Chip	100-500	30	[7]
Fe_3O_4 MNPs	50-1000	30	[8]
Au @ Ag NRs	50-20000	39	[9]
N–GQDs	25-375	16	[10]
H_2TCPP-NiO	50-500	20	[11]
mesoporous ceria	200-1000	10	[12]
$V_2C@VO_x$	0.1-3000	0.08	This work

Tab. S5. Determination of glucose in human serum.

Samples	Determination (μM)	Added (μM)	Detected (μM)	Recovery (%)	RSD (%) (n=3)
		9.00	31.9	97	1.4
I	23.6	18.00	39.7	91.9	0.8
		27.00	49.9	97.3	1.9
		9.00	38.4	104	4
II	28.3	18.00	45.4	96.8	3.2
		27.00	54.3	96.6	4.9
		9.00	77.6	97.3	4.2
III	70.5	18.00	84.6	99.3	1.3
		27.00	94	95	3.1

Reference

1. Y. He, X. Li, X. Xu, J. Pan and X. Niu, *J. Mater. Chem. B*, 2018, 6, 5750-5755.
2. A. Caliò, P. Dardano, V. Di Palma, M. F. Bevilacqua, A. Di Matteo, H. Iuele and L. De Stefano, *Sensor. Actuat. B-Chem*., 2016, 236, 343-349.
3. L. Feng, B. Liu, R. Xie, D. Wang, C. Qian, W. Zhou, J. Liu, D. Jana, P. Yang and Y. Zhao, *Adv. Funct. Mater.*, 2021, 31, 2006216.
4. D. Liu, C. Ju, C. Han, R. Shi, X. Chen, D. Duan, J. Yan and X. Yan, *Biosens. Bioelectron*., 2021, 173, 112817.
5. L. Zhang, Z. Liu, Q. Deng, Y. Sang, K. Dong, J. Ren and X. Qu, *Angew. Chem. Int. Edit*., 2021, 60, 3469-3474.
6. C. Fang, Z. Deng, G. Cao, Q. Chu, Y. Wu, X. Li, X. Peng and G. Han, *Adv. Funct. Mater*., 2020, 30, 1910085.

7 J. Xiao, Y. Liu, L. Su, D. Zhao, L. Zhao and X. Zhao, *Anal. Chem*., 2019, 91, 14803-14807.

8 L. Gao, J. Zhuang, L. Nie, J. Zhang, Y. Zhang, N. Gu, T. Wang, J. Feng, D. Yang, S. Perrett, et al. *Nat. Nanotechnol*., 2007, 2, 577-583.

9 L. Han, C. Li, T. Zhang, Q. Lang and A. Liu, ACS. *Appl. Mater. Inter*., 2015, 7, 14463-14470.

10 L. Lin, X. Song, Y. Chen, M. Rong, T. Zhao, Y. Wang, Y. Jiang and X. Chen, *Anal. Chim. Acta*., 2015, 869, 89-95.

11 Q. Liu, Y. Yang, H. Li, R. Zhu, Q. Shao, S. Yang and J. Xu, *Biosens. Bioelectron*., 2015, 64, 147-153.

12 M. S. Kim, J. Lee, H. T. Ahn, M. L. Kim and J. Lee, *Nanoscale*, 2020, 12, 1419-1424.